Scaling of Taylor flow in small square channels of different size

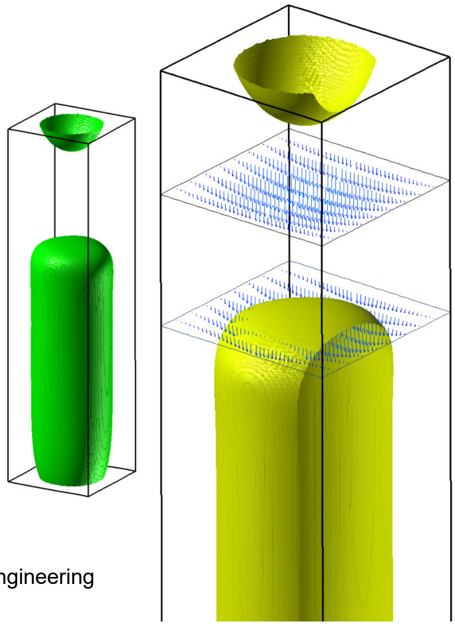

Martin Wörner

Karlsruhe Institute of Technology
Institute for Nuclear and Energy Technologies

1st Int. Conf. Multiscale Multiphase Process Engineering
Kanazawa, Japan, October 4-7, 2011

Content

Monolith reactors

- Ceramic block with hundreds of straight parallel channels
- Various cross-sectional shapes, often square
- Hydraulic diameter is typically in the range 0.5 – 5 mm
- Coated with a catalytically active layer (washcoat)
- Most prominent application: catalytic converter in cars for exhaust gas cleaning

Boger et al. 2004

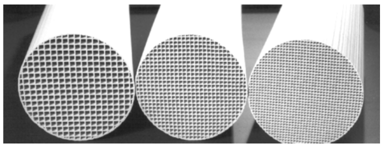

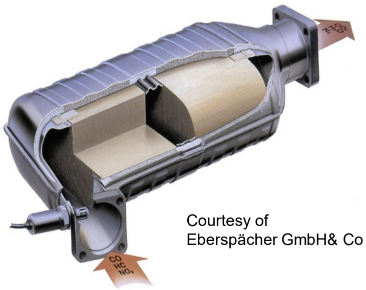

Courtesy of Eberspächer GmbH& Co

Multiphase monolith reactors

- Attractive for heterogeneously catalyzed gas-liquid reactions
  - e.g. Fischer-Tropsch synthesis
- Advantages of Taylor flow (TF)
  - Thin liquid film (bubble-wall)
  - Large specific interfacial area
  - Recirculation within the segmented liquid slugs
  - Unique combination of good mass transfer properties and reduced axial dispersion
- Here: Study influence of channel size on Taylor flow hydrodynamics

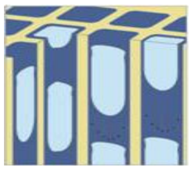

Kreutzer, Moulijn

TF in square channel, D_h=1 mm

TECHNISCHE UNIVERSITÄT DRESDEN

(Tobias Bauer, Rüdiger Lange)

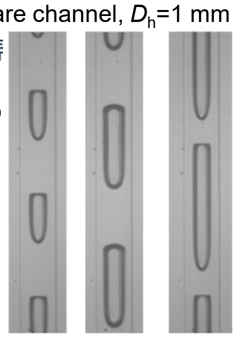

Literature survey

- Hydrodynamic properties of Taylor flow (e.g. the liquid film thickness δ_F/D_h) are correlated in terms of the capillary number $Ca = \mu_L U_B/\sigma$ which does not involve a length scale
- Numerical studies* for inviscid Taylor bubbles (in plane or circular channels) indicate a certain non-linear influence of the Reynolds number $Re = \rho_L U_B D_h/\mu_L$ on δ_F/D_h and the shape of the front and rear meniscus
- A change of D_h modifies both Re and the Eötvös number $E\ddot{o} = g(\rho_L - \rho_G)D_h^2/\sigma$ (i.e. the relative importance of buoyancy)
- Here we study the <u>overall effect</u> of a change of the channel size on hydrodynamic properties of co-current downward Taylor flow in a square channel (with a viscous gas phase)

* Heil (2001), Giavedoni & Saita (1999), Kreutzer (2003)

Content

- Introduction
  - Monolith reactors and Taylor flow
- Numerical simulation of Taylor flow
  - Method and computational set-up
  - Validation
- Results for different hydraulic diameters
  - Comparison of bubble shape
  - Scaling of bubble velocity, bubble diameter, specific interfacial area
- Conclusions and outlook

Simulation method*

- Governing equations
  - Navier-Stokes equation in single field formulation with surface tension term for two incompressible immiscible Newtonian fluids with constant physical properties
- Numerical method
  - Volume-of-fluid method with PLIC reconstruction
  - Finite volume discretization on a staggered 3D Cartesian grid
  - Projection method for pressure-velocity coupling
  - Explicit 3rd order Runge-Kutta time integration scheme
  - In-house computer code TURBIT-VOF

* for details see Öztaskin et al. Phys. Fluids **21** (2009) 042108

Computational set-up for Taylor flow

- Set-up
  - co-current downward flow of squalane ($C_{30}H_{62}$) and nitrogen
  - square channel (hydraulic diameter D_h)
  - consideration of **one unit cell**
  - periodic boundary conditions in vertical (axial) direction
- Prescribed parameters
  - gas content: ε_G = 0.2 or 0.4
  - unit cell length: L_y / D_h = 4 or 6 (grid up to 80 × 480 × 80 cells)
  - pressure drop across the unit cell $Eu_{ref} = \Delta p_{uc} / (\rho_L U_{ref}^2)$

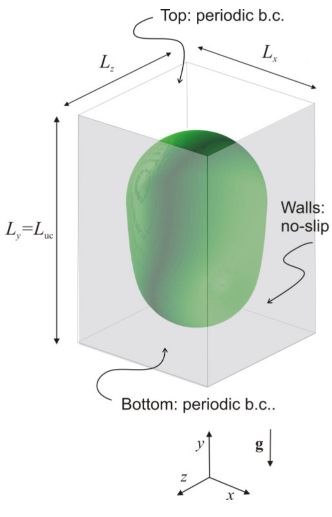

Evolution in time

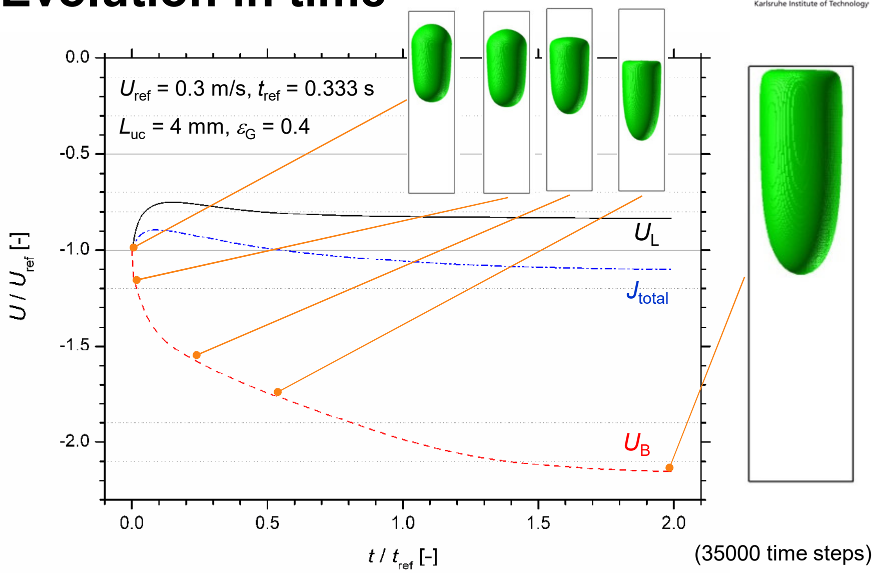

(35000 time steps)

Experimental validation*

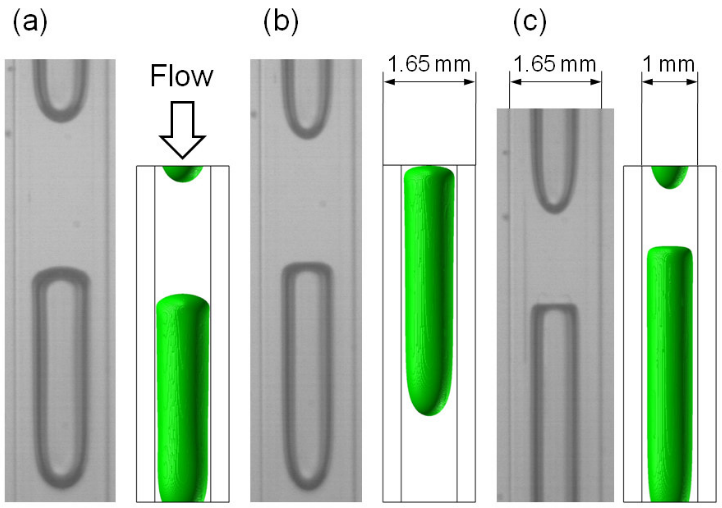

Keskin et al. AIChE J. **56** (2010) 1693–1702

* Experiments by T. Bauer and R. Lange

TECHNISCHE UNIVERSITÄT DRESDEN

Content

- Introduction
  - Monolith reactors and Taylor flow
- Numerical simulation of Taylor flow
  - Method and computational set-up
  - Validation
- Results for different hydraulic diameters
  - Comparison of bubble shape
  - Scaling of bubble velocity, bubble diameter, specific interfacial area
- Conclusions and outlook

Fixed simulation parameters

- Non-dimensional unit cell length $L_{uc} / D_h = 4$
- Gas hold-up in unit cell $\varepsilon = 0.4$
- Phys. properties squalane-nitrogen (20°C, 20 bar)
  - Liquid density $\rho_L = 802$ kg/m^3
  - Gas density $\rho_G = 23.6$ kg/m^3
  - Liquid viscosity $\mu_L = 0.029$ Pa s
  - Gas viscosity $\mu_G = 0.01804$ mPa s
  - Coefficient of surface tension $\sigma = 0.0286$ N/m
  - Liquid-to-gas density ratio $\rho_L / \rho_G = 34$
  - Liquid-to-gas viscosity ratio $\mu_L / \mu_G = 1607$
  - Morton number $Mo = 3.6 \times 10^{-4}$

Simulation cases

D_h [mm]	La [-]	$Eö$ [-]	Π_y [-]	U_B [m/s]	J_{tot} [m/s]	Ca [-]	Re [-]
0.5	13.64	0.067	-6	0.112	0.074	0.114	1.55
0.5	13.64	0.067	-7	0.147	0.093	0.149	2.03
0.5	13.64	0.067	-8	0.200	0.120	0.202	1.67
0.5	13.64	0.067	-9	0.260	0.149	0.263	3.59
0.5	13.64	0.067	-10	0.329	0.181	0.334	4.55
0.5	13.64	0.067	-11	0.411	0.217	0.417	5.68
0.5	13.64	0.067	-12	0.493	0.254	0.500	6.82
1	27.27	0.267	-5	0.257	0.149	0.261	7.11
1	27.27	0.267	-6	0.379	0.207	0.385	10.49
2	54.55	1.068	-2.9	0.179	0.114	0.181	9.89
2	54.55	1.068	-3.1	0.210	0.130	0.213	11.60
2	54.55	1.068	-3.3	0.243	0.147	0.247	13.45

$$La = \frac{\sigma \rho_L D_h}{\mu_L^2}$$

$$Eö = \frac{g(\rho_L - \rho_G) D_h^2}{\sigma}$$

$$\Pi_y = Eu_{ref} \frac{L_{uc}}{D_h} - Fr_{ref}$$

$$Eu_{ref} = \frac{\Delta p_{uc}}{\rho_L U_{ref}^2}$$

$$Fr_{ref} = \frac{U_{ref}^2}{g L_{ref}}$$

$$Ca = \frac{\mu_L U_B}{\sigma}$$

$$Re = \frac{\rho_L D_h U_B}{\mu_L} = La \cdot Ca$$

$$U_{ref} = 0.12\,\text{m/s}, \quad L_{ref} = D_h$$

Bubble shapes for D_h = 0.5 mm

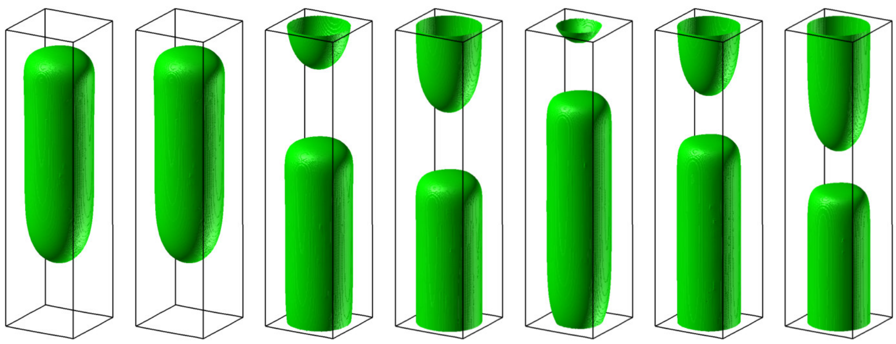

Increase of Ca and $Re = La\,Ca$

Increase of δ_F, L_B, κ_{front} (curvature of front meniscus)
Decrease of D_B, L_{slug}, κ_{rear} (curvature of rear meniscus)

Comparison of bubble shapes

- Case ANB_E_0005_E
  $D_h = 0.5$ mm
  $Ca = 0.202$
  $Re = 1.7$
  $Eö = 0.067$
- Case ANB_E_002_B
  $D_h = 2.0$ mm
  $Ca = 0.213$
  $Re = 11.6$
  $Eö = 1.068$

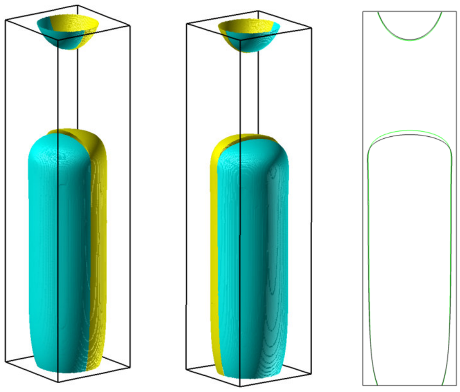

- Combined influence of Re and $Eö$ for fixed value of Ca
  - very small influence on δ_F/D_h and $\kappa_{front} D_h$
  - notable influence on $\kappa_{rear} D_h$ (inertial effect, known in literature)

Non-dimensional bubble velocity

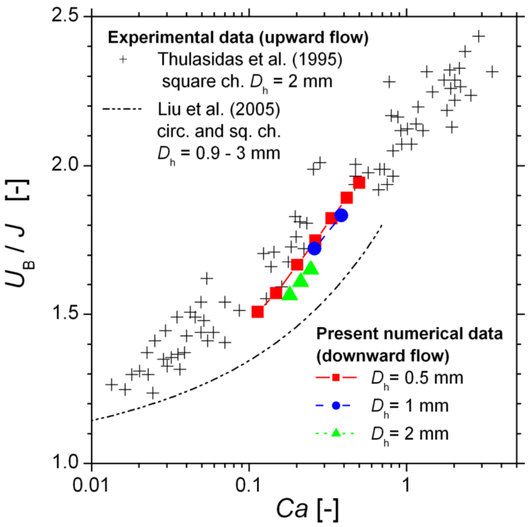

- The ratio U_B / J slightly decreases with increase of D_h
- This is most probably an effect of buoyancy
- For downward flow the buoyancy force acts opposite to the applied pressure gradient force so that with increase of $Eö$ the bubble slows down relative to the total superficial velocity J

Non-dimensional bubble diameter

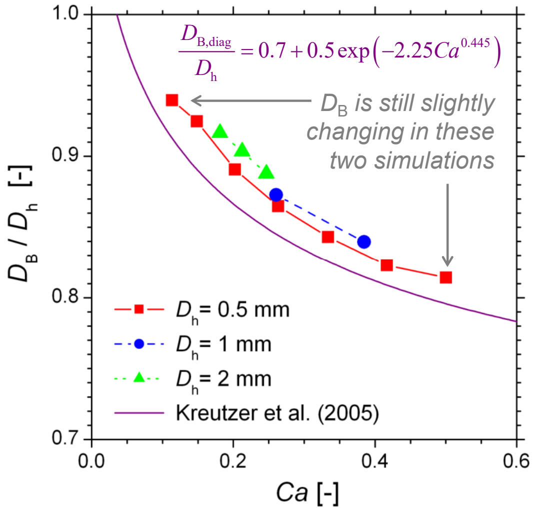

- The ratio D_B / D_h slightly increases with increase of D_h (i.e. the liquid film thickness decreases)
- The correlation of Kreutzer slightly underestimates the numerical values of D_B / D_h but can easily be adapted (e.g. change 0.5 to 0.56)

Non-dimensional interfacial area

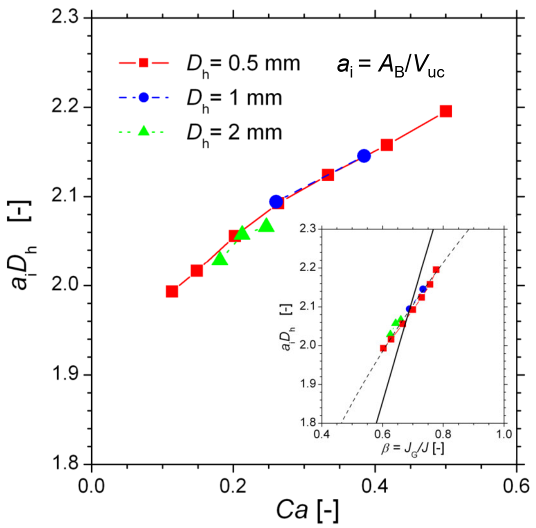

- The influence of *Re* and *Eö* on the non-dimensional specific interfacial area $a_i D_h$ is negligible
- There exists no literature correlation for $a_i D_h$ as function of *Ca*
- The correlation of Keskin et al. (2010) $a_i D_h = 2.9\beta^{0.875}$ (solid line) yields a wrong slope (dashed line: $a_i D_h = 2.41\beta^{0.38}$)

Content

Conclusions

- Appropriately normalized hydrodynamic properties of Taylor flow in square mini-channels of different size scale with the capillary number
- The influence of the Reynolds number and Eötvös number is in general small (al least for $D_h \leq 2$ mm)
  - negligible influence on non-dimensional interfacial area
  - slight influence of *Re* on curvature of rear meniscus
  - slight influence of *Eö* on ratio U_B / *J* for downward flow
- These findings indicate that a transfer of exp. Or numerical results obtained for a certain value of D_h to smaller/larger channels is possible

Outlook

- Further simulations
  - for $D_h = 1$ and 2 mm at higher/smaller values of Ca
  - simulations for $D_h = 4$ mm
  - other fluid properties (influence of Laplace number)
- Development of general quantitative scaling relations in terms of *Ca* with corrections that account for the influence of *Re*, *Eö*, *La*

- Acknowledgements
  - A. Boran, Sakarya University, Turkey
  - DFG grant WO 1682/1-1 (SPP 1506)

Backup Slides

Displacement of liquid by an inviscid gas

- Inertial effects on liquid film thickness in 2D (planar) Bretherton problem (numerical results, inviscid bubble)

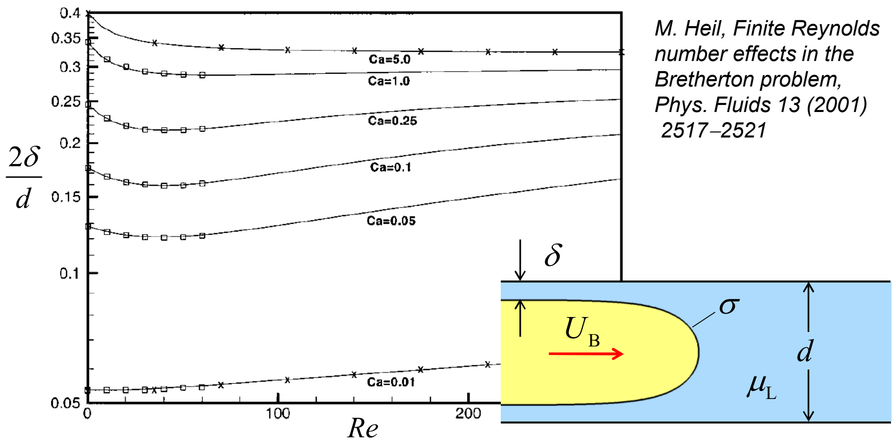

M. Heil, Finite Reynolds number effects in the Bretherton problem, Phys. Fluids 13 (2001) 2517–2521

Shape of the rear meniscus

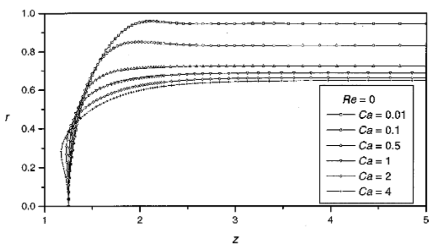

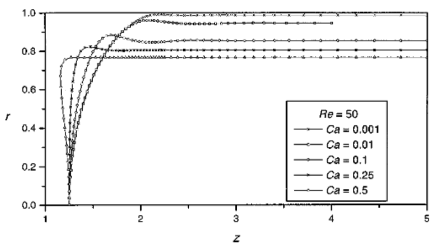

Numerical study (inviscid bubble)

M.D. Giavedoni, F.A. Saita, The rear meniscus of a long bubble steadily displacing a Newtonian liquid in a capillary tube, Phys. Fluids 11 (1999) 786–794

- The rear meniscus shows a complex shape depending on the values of *Ca* and *Re*
- Of primary influence is the value of the capillary number

Bubble shape – effect of *Re*

M. Kreutzer, Ph.D thesis, Delft University of Technology, 2003

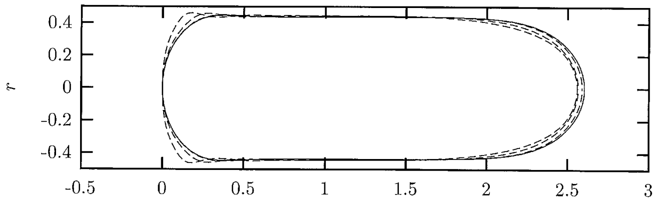

Figure 2.9: Shape of the gas–liquid interface for $Re = 1, 10, 100, 200$ at $Ca = 0.04$

- *Re* and *Ca* are linearly related by the Laplace number *La*

$$Re = La \cdot Ca, \qquad La \equiv \frac{\sigma \rho_L D_h}{\mu_L^2}$$

- For a given fluid pair and channel size a change in *Ca* goes along with a change in *Re*

Experiments of TECHNISCHE UNIVERSITÄT DRESDEN (T. Bauer, R. Lange)

(Pressure = 20 bar)

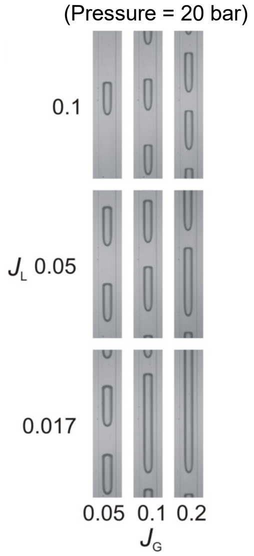

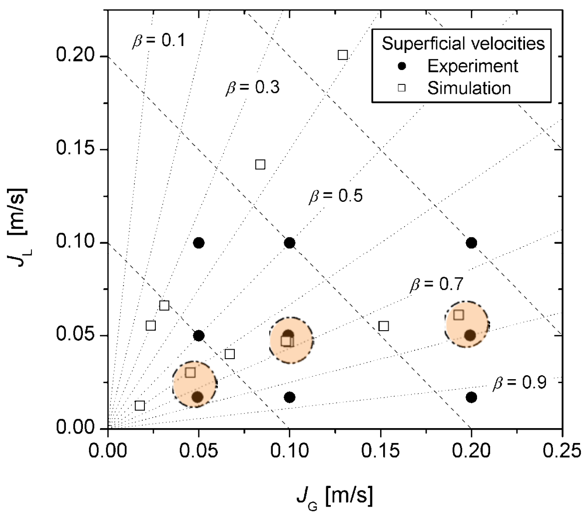

Steady bubble shape at different *Ca*

$1\,\mathrm{mm} \times 1\,\mathrm{mm}$

$L_{\mathrm{uc}} = 6\,\mathrm{mm}$

$\varepsilon_{\mathrm{G}} = 0.4$

$$\frac{Re}{Ca} = \frac{\sigma \rho_{\mathrm{L}} D_{\mathrm{h}}}{\mu_{\mathrm{L}}^2} \equiv La = 27.27$$

$$Ca \equiv \frac{\mu_{\mathrm{L}} U_{\mathrm{B}}}{\sigma}$$

$$Re \equiv \frac{\rho_{\mathrm{L}} D_{\mathrm{h}} U_{\mathrm{B}}}{\mu_{\mathrm{L}}}$$

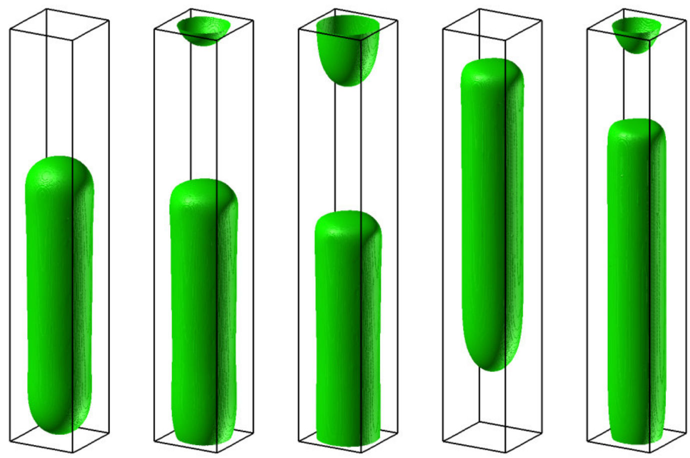

Ca =	0.045	0.12	0.17	0.26	0.49
Re =	1.22	3.19	4.64	7.16	13.4

Simulation cases

D_h [mm]	*La* [-]	*Eö* [-]	Π_y [-]	U_B [m/s]	J_{tot} [m/s]	*Ca* [-]	*Re* [-]	Case	NTIM
0.5	13.64	0.067	-6	0.112	0.074	0.114	1.55	ANB_O_0005_A	334000
0.5	13.64	0.067	-7	0.147	0.093	0.149	2.03	ANB_O_0005_D	378000
0.5	13.64	0.067	-8	0.200	0.120	0.202	1.67	ANB_E_0005_E	296000
0.5	13.64	0.067	-9	0.260	0.149	0.263	3.59	ANB_E_0005_D	272000
0.5	13.64	0.067	-10	0.329	0.181	0.334	4.55	ANB_E_0005_B	224000
0.5	13.64	0.067	-11	0.411	0.217	0.417	5.68	ANB_O_0005_B	314000
0.5	13.64	0.067	-12	0.493	0.254	0.500	6.82	ANB_O_0005_C	250000
1	27.27	0.267	-5	0.257	0.149	0.261	7.11	TUD_SQUA_E	122000
1	27.27	0.267	-6	0.379	0.207	0.385	10.49	TUD_SQUA_O	140000
2	54.55	1.068	-2.9	0.179	0.114	0.181	9.89	ANB_E_002_D	270000
2	54.55	1.068	-3.1	0.210	0.130	0.213	11.60	ANB_E_002_B	180000
2	54.55	1.068	-3.3	0.243	0.147	0.247	13.45	ANB_E_002_C	272000